Analysis of XPS and AES of Carbon Allotrope (Diamond, Graphite, C_{60}) by DFT Calculations using the Model Molecules

S. Koizumi, T. Otsuka[1], K. Endo*[1], and T. Morohashi

ULVAC-PHI INC., Chigasaki 253-0084, Kanagawa, Japan
[1]Department of Chemistry, Faculty of Science,Kanazawa University, Kanazawa 920-1192, Ishikawa, Japan
**endo@wriron1.s.kanazawa-u.ac.jp*

(Received January 18, 2002; accepted May 9, 2002)

X-ray photoelectron, and Auger electron spectra of diamond, graphite, and C_{60} fullerene have been analyzed by deMon density-functional theory (DFT) calculations using the model adamantane derivative ($C_{10}H_{12}(CH_3)_4$), pyrene ($C_{16}H_{10}$), and C_{60} molecules, respectively. The theoretical valence photoelectron, and Auger electron spectra for the allotrope show good accordance with the experimental ones, although we couldn't also observe the Auger electron spectrum for solid C_{60}. The experimental AES of the allotrope can be classified in each range of 1s-2p2p, 1s-2s2p, and 1s-2s2s transitions for C KVV spectra.

Introduction

The carbon allotropic forms of diamond, graphite, and fullerene differ in their physical and chemical properties because of differences in the arrangement and bonding of tetrahedral sp^3, planer sp^2, and caged sp^2 carbons, respectively. Although the difference of the structure between the allotrope will be reflected in the spectra by several analytical methods (X-ray photoelectron, emission, and Auger electron spectroscopy, NMR, IR and so on), there was no work that has dealt with such difference. Recently in the previous works[1, 2], we analyzed the valence X-ray photoelectron and emission spectra (XPS and XES) of diamond and graphite by deMon density-functional theory (DFT) program[3] using the model molecules. In the work, we showed that the combined analysis of the XPS and C Kα XES enables in dividing the observed valence electronic distribution into the individual contributions for pσ-, and pπ-bonding MOs of the allotrope.

In the present work, our aim is to perform the determination for analysis of the photoelectron, and Auger electron spectra of the allotrope by the DFT calculations, although we couldn't also observe the Auger electron spectrum for solid C_{60}. Here we demonstrate the combination analysis of the valence XPS, and AES for the allotrope (diamond, graphite and fullerene) by deMon DFT calculations using the model adamantane derivative ($C_{10}H_{12}(CH_3)_4$), pyrene ($C_{16}H_{10}$) and C_{60} molecules, respectively.

Theoretical Background

In order to explain solid-state effect, we define a quantity *WD* as stated in early works.[4-8] This quantity *WD* denotes the sum of the work function of the sample (*W*) and other energy effects (*D* as *delta*), such as the polarization energy, the width of the intermolecular band formation, and the peak broadening in the solid state. The experimental *WD*s can be estimated from differences between theoretical core-electron binding energies (CEBE)s of model molecules, and experimental binding energies of the allotrope. Therefore, for the comparison between the calculated CEBEs for single molecules of cluster model and experimental CEBEs of solid allotrope, we must shift each computed CEBE (or vertical ionization potential (VIP)) I'_k by a quantity *WD* as $I_k(I_{FL}) = I'_k - WD$, to convert to CEBE (or VIP) $I_k(I_{FL})$ relative to the Fermi

level.

a) CEBEs, VIPs, and Auger electron energies

The Slater's transition-state (TS) method[9] was introduced by considering an electronic process of ionization or excitation at fixed molecular geometry. Williams and co-workers[10] proposed the extension of Slater's transition state method, which is called as the generalized transition state (GTS) method. The endothermicity is approximated as

$$\Delta E = E(1) - E(0) = E_1 + E_2 + E_3 + E_4 + , \quad (1)$$

by

$$\Delta E \approx \frac{F(0)+3F(2/3)}{4} = E_1 + E_2 + E_3 + \frac{8}{9}E_4 + \ldots , \quad (2)$$

where $F(\lambda) = \partial E(\lambda)/\partial\lambda$, $E(\lambda) = S\lambda^k E_k$, and λ ($0 = \lambda = 1$) is assumed to be a continuous variable. $E(0)$ and $E(1)$ denote the energies of the initial and final states, respectively. For the ionization of an electron from molecular orbital (MO) ϕ_k of interest, λ represents the fraction number of electron removed from the Kohn-Sham (KS) MO. According to Janak theorem[11], $F(\lambda)$ becomes the negative KS orbital energy, $e_k(\lambda)$. For the calculation of CEBEs, this procedure is applied in the following way. In the unrestricted generalized transition state (uGTS) method, we removed the 2/3 electron from the inner core-electron level KS MO ϕ_k.

Following Chong[12-15], the relativistic correction (C_{rel}) for carbon to fluorine is added to the computed CEBEs:

$$C_{ref} = KI_{nr}^{N} , \quad (3)$$

where $K = 2.198\times10^{-7}$, $N = 2.178$, and I_{nr} is the non-relativistic CEBE.

For the VIPs of the valence regions, we introduced the restricted generalized diffuse ionization (rGDI) model[16], which is just the extension of the restricted diffuse ionization (rDI) model that Åsbrink and co-workers proposed in the HAM/3 method[17]. In the rGDI model, as indicated in our previous work,[16] the 2/3 electron is removed evenly from all α and β electron valence MOs and the negative resulting orbital energies are approximated as each $F(2/3)$ for each valence MO. Thus, we obtain each valence VIP using Eq. (2).

The calculation of Auger electron energy may be expressed in terms of the single hole ionization energy for an electron in the core orbital, I_c at the initial state, and the double hole ionization energy in the valence orbital, $I_{VV'}$ at the final state. The $I_{VV'}$ is often expressed as the sum of two single ionization energies and the correction terms. We can then give the Auger electron energy in the following way,

$$E_{cjk} = I_c - I_j - I_k^* - WDC , \quad (4)$$

where I_c and (I_j, I^*_k) denote the CEBE and VIPs, respectively. The WDC involves the work function, other energy effects and the correction terms. For the calculation of VIP, I^*_k, we used the restricted diffuse ionization (rDI) model in the N – 1 electron system. Therefore, one and half of electrons are removed evenly from all the valence MOs in neutral molecule and the negative of the resulting orbital energies correspond to calculated VIP's, I^*_k.

b) Intensity of valence XPS, and AES

The intensity of valence XPS was estimated from the relative photoionization cross-section for Al $K\alpha$ radiation using the Gelius intensity model[18]. For the relative atomic photo-ionization cross-section, we used the theoretical values from Yeh[19].

The Auger transition probability from an initial core hole to the final state with two holes in valence region and an electron in the continuum was expressed by Wentzel[20],

$$M_{CVV'} = \sum_{\varepsilon} |< \Psi(c, \varepsilon) | \sum_{i,j} \frac{1}{r_{ij}} | \Psi(v, v') > |^2 . \quad (5)$$

Here $\Psi(c, \varepsilon)$ is the total wavefunction which denotes the core hole c, and final-state continuum ε orbitals, respectively; the other total wavefunction $\Psi(v, v')$ involves the two final-state hole orbitals in valence levels.

For the relative Auger transition intensity of

the simple gas molecules, Siegbahn and co-workers had derived approximate formulae using molecular orbital (MO) calculations with a linear combination of atomic orbitals[21] under the assumption of intra-atomic transition. On the other hand, Ramarker and co-workers[22, 23] proposed the one-center intensity model for the calculation of Auger electron intensities of solid SiO_2. The relative Auger intensities are given as

$$M_{cjk} = N' \sum_{\mu,\nu} |C_{\mu j}|^2 |C_{\nu k}|^2 P_{c\mu\nu} \quad . \qquad (6)$$

Here $|C_{\mu j}|^2$ and $|C_{\nu k}|^2$ represent the electron density populations of the atomic orbitals, ψ_μ and ψ_ν, respectively, on the central atom A associated with the molecular orbitals, ϕ_j and ϕ_k. N' and $P_{c\mu\nu}$ denote a statistical factor and the appropriate weighted subshell Auger transition probabilities, respectively. For the subshell Auger transition probabilities, we used the theoretical values from Chen and co-workers[24].

Calculation Details

The model molecules [adamantane derivative ($C_{10}H_{12}(CH_3)_4$), pyrene ($C_{16}H_{10}$), and fullerene C_{60}] were calculated by the deMon-KS DFT program[3]. For the geometry of the molecules, we used the optimized cartesian coordinates from the semiempirical AM1 (version 6.0) method[25].

The deMon calculations were performed with the exchange-correlation potential labeled as B88/P86, made from Becke's 1988 exchange functional[26] and Perdew's 1986 correlation functional[27]. In the program, we used a non-random grid and a polarized valence double-ς (DZVP) basis of (621/41/1*) for C, and (41) for H with auxiliary fitting functions labeled (4, 4; 4, 4) for C, and (3, 1; 3, 1) for H.

To simulate the valence XPS of carbon allotrope theoretically, we constructed from a superposition of peaks centered on each VIP, I_k. As was done in previous works[6-10], each peak was represented by a Gaussian curve. In the case of the linewidth ($WH(k)$), we used $WH(k) = 0.10\ I_k$ (proportional to the ionization energy) for valence XPS.

In the calculations of the CEBEs, we used a polarized valence double-ς (DZVP)) basis set for the model molecules in the initial state and the scaled polarized valence double-ς (DZVP) basis set in the uGTS model.

In order to simulate the AES of the carbon allotrope, we constructed from a superposition of peaks centered on the Auger electron energies, $[(\text{CEBE}, I_c^A)_{1s} - (\text{VIP}, I_j) - (\text{VIP}', I^*_k)]$ in each central atom A on the assumption that Auger process dominated by the intra-atomic transition. Each peak was represented by Gaussian lineshape functions of a fixed linewidth 3 eV(experimental resolution) for the AES.

Experimental

We used a diamond film as deposited from gas-phase mixture containing hydrogen, graphite as produced by pyrolysis, and commercially available fullerene C_{60} (Aldrich chemical Co. Inc), respectively.

The experimental photoelectron and Auger electron spectra of the samples were obtained on a PHI 5400 MC ESCA spectrometer, using monochromatized Al Kα radiation. We couldn't obtain the Auger electron spectrum of the fullerene due to the charging effect on the surface of the sample. The spectrometer was operated at an X-ray Al Kα source power of 600 W (15 kV × 40 mA). The photon energy was 1486.6 eV. A pass energy of 35.75 eV was employed for high resolution scans in a valence-band analysis (50 eV of range). The angle between the X-ray source and the analyzer was fixed at 45°. The size in the measurement was 3 × 1 mm^2.

The use of dispersion compensation yielded an instrumental resolution of 0.5 eV with the full width at half-maximum on the Ag 3d line of silver. Multiple-scan averaging on a multi-channel analyzer was used for the valence band region, although a very low photoelectron emission cross-section was observed in this range.

Gold of 20 Å thick was deposited on the film (or disc) of the samples using an ion sputter unit (Hitachi E 1030) for scanning electron microscope.

A low-energy electron flood gun was used in order to avoid any charging effect on the surface of the sample. We used the Au 4f core level of the gold decoration membrane (or disc) as a calibration reference.

Results and Discussion

Diamond films are desired for many applications[28], including wear-resistant coatings, thin film semiconductor devices, X-ray lithographic membranes, and durable infrared windows. For the graphite, it is well-known that the material is produced especially as very strong fibers by pyrolysis, at 1500 °C or above, of oriented organic polymer fibers. When incorporated into plastics, the reinforced materials are light and very strong. In the case of fullerene C_{60}, we expect the materials will be applied in lubrication, coating, non-linear optical and electronic device, since the synthesis of the macroscopic quantities[29] and the surface modification[30] have been performed.

Although the electronic states of diamond[31, 32] and graphite[33] were investigated from analysis of valence XPS and XES using band theory of the one-electron partial density of states (DOS), the workers[31-33] did not sufficiently explain the electronic orbital nature of each peak for the experimental spectra of diamond and graphite. As so far as we know, no one currently still demonstrated the analysis of AES of the carbon allotrope from theoretical viewpoints. In this section, we perform the detailed analysis for valence XPS and AES of the diamond, graphite, and fullerene by deMon DFT calculations using the model molecules.

Table 1. Observed peak, VIP, main AO photo-ionization cross-section, orbital nature and functional group for X-ray photoelectron spectra of carbon allotrope

observed peak (eV)	VIP (eV)	main AO photo-ionization cross-section	orbital nature	functional group
diamond				
19.0(16.0-23.0)[a]	20.24-24.32	C2s	sσ(C2s-C2s)-B	-C(f)-C(f)
15.0(13.0-16.0)[a]	18.59-18.91	C2s	sσ(C2s-C2s)-B	-C(f)-C(f), -C(f)-C(p)
10.0{shoulder	15.66-16.34	C2s	pσ(C2s-C2p)-B	-C(f)-C(f), -C(f)-C(p)
peak(2.0-12.0)[a]}	13.01-13.78	C2p	pσ(C2p-C2p)-B	-C(f)-C(p)
	8.60-12.65	C2p	pσ(C2p-C2p)-B	-C(f)-C(f), -C(f)-C(p)
graphite				
16.0(13.0-23.0)[a]	19.88-24.67	C2s	sσ(C2s-C2s)-B	-C=C
12.5(10.5-13.0)[a]	17.35-17.83	C2s	s, pσ(C2s-C2s,p)-B	-C=C
10.0{shoulder	13.76-15.64	C2p	pπ(C2p-C2p)-B	-C=C
peak(2.0-10.5)[a]}	7.30-12.53	C2p	pπ (C2p-C2p)-B	-C=C
fullerene				
18.0(15.0-24.0)[a]	23.08-26.36	C2s	sσ(C2s-C2s)-B	-C=C
14.0(12.0-15.0)[a]	19.53-21.75	C2s	s, pσ(C2s-C2s,p)-B	-C=C
11.0(10.0-12.0)[a]	17.35-18.56	C2s,C2p	pσ, π(C2s,p-C2p)-B	-C=C
8.0(6.0-10.0)[a]	13.38-15.80	C2p	pπ(C2p-C2p)-B	-C=C
5.0(4.0-6.0)[a]	9.76-13.00	C2p	pπ(C2p-C2p)-B	-C=C
3.0(1.0-4.0)[a]	7.63-9.50	C2p	pπ (C2p-C2p)-B	-C=C

[a] shows the peak range. WD(difference between calculated and observed peaks) = 5.5eV. Notations, -B, -C(f) and -C(p) denote bonding, frame and pendant carbons, respectively.

a) diamond

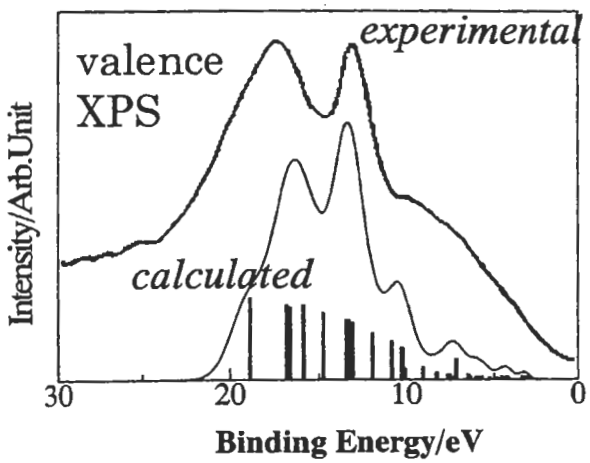

b) graphite

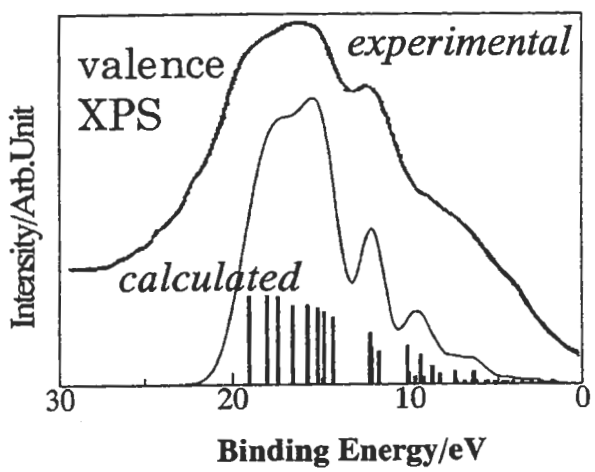

c) C_{60}

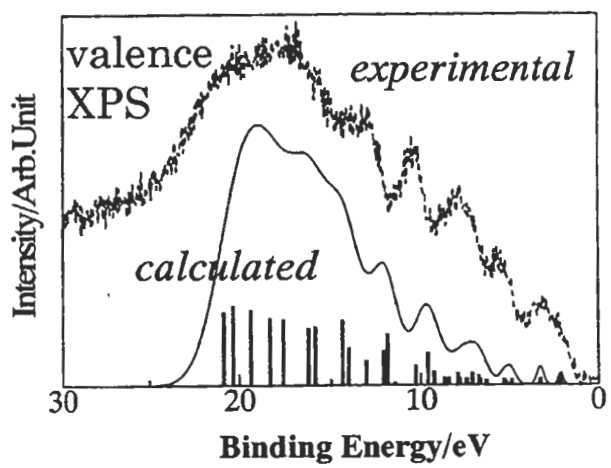

Fig. 1. Experimental and calculated valence X-ray photoelectron spectra of carbon allotrope, *a)* diamond, *b)* graphite, and *c)* fullerene

1) **XPS of the carbon allotrope**

In Fig. 1 ***a) ~ c)***, X-ray photoelectron spectra reflect the differences of the chemical structures among diamond, graphite and fullerene, respectively. The simulated spectra by DFT calculations using the model molecules [adamantane derivative ($C_{10}H_{12}(CH_3)_4$), pyrene ($C_{16}H_{10}$) and fullerene (C_{60})] show good accordance with the experimental ones. The spectrum of diamond has double strong peaks due to the sσ (C2s-C2s) bonding in the energy range of 10 – 20 eV, while that of graphite shows a broader strong peak owing to the sσ (C2s-C2s) bonding in the range of 14 – 20 eV and the middle intensive shoulder peak due to the pσ (C2s-C2p) and pπ (C2p-C2p) bondings at around 12 eV. For the fullerene, the experimental spectrum in the range of more than 12 eV is almost similar to that of graphite, although it is characteristic that the spectrum in the range of less than 12 eV has four broader peaks mainly due to the pπ (C2p-C2p) bondings. In Table 1, we showed the observed peaks and calculated VIPs, main contributions of atomic orbital photo-ionization cross-section, orbital nature and the functional groups for valence X-ray photoelectron spectra of the carbon allotrope.

2) **AES of the carbon allotrope**

For Auger electron spectra of the carbon allotrope in Fig. 2 ***a) ~ c)***, we plotted the intensity versus the energy scale using the differences between incident X-ray energy Al Kα (1486.7 eV) and the Auger electron energies, $[(\mathrm{CEBE}, I_c^A)_{1s} - (\mathrm{VIP}, I_j) - (\mathrm{VIP}', I^*_k)]$ in each central atom A. In the figures, the simulated AES for diamond, graphite and fullerene show good accordance with the experimental spectra, although we couldn't also observe the Auger electron spectrum for solid C_{60}. In simulated spectra of the figure, we showed total carbon KVV AES with solid lines and the individual 1s-2p2p, 1s-2s2p, and 1s-2s2s transition spectra with dashed lines, respectively. We can see a characteristic difference of simulated carbon KVV AES in the kinetic energy range of 235 –275 eV among diamond, graphite and fullerene in Fig. 3. The simulated peaks for fullerene and graphite seem

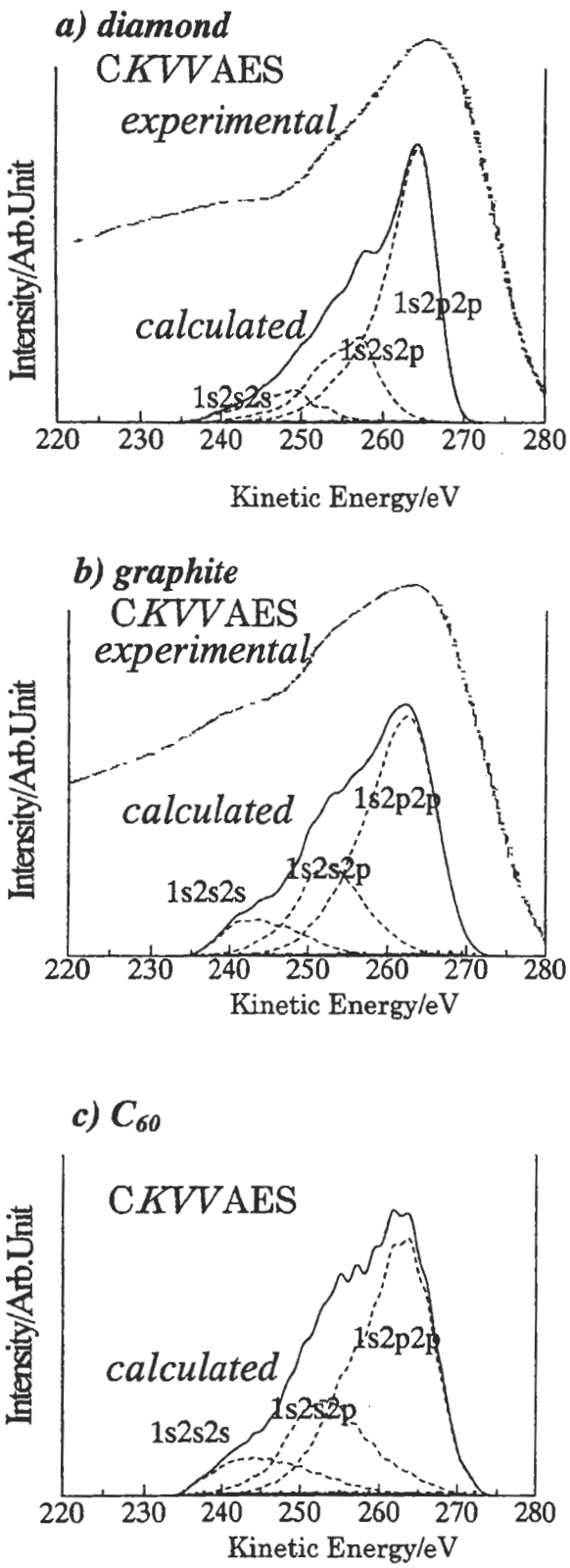

Fig. 2. Experimental and calculated carbon KVV Auger electron spectra of carbon allotrope, *a)* diamond, *b)* graphite, and *c)* fullerene

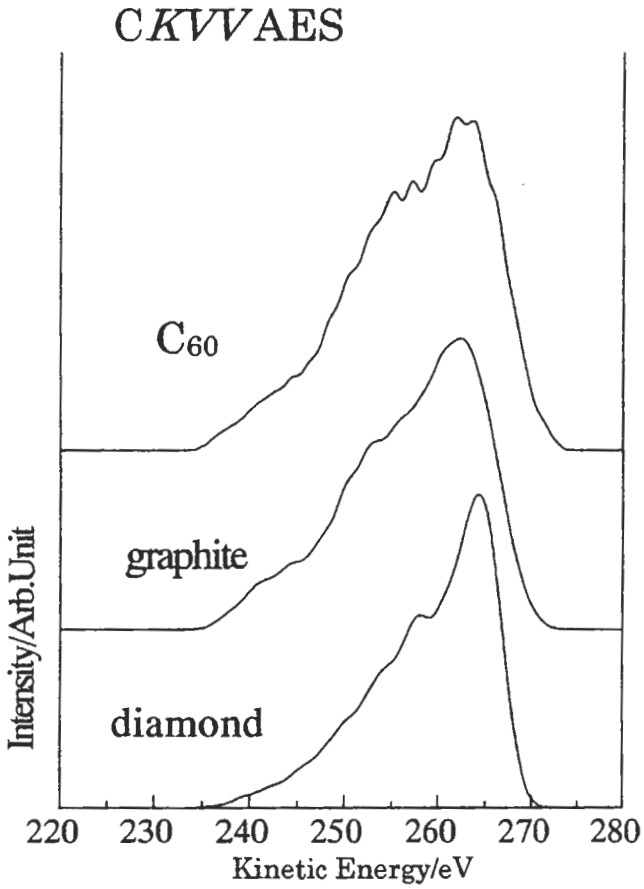

Fig. 3. Calculated carbon KVV Auger electron spectra of diamond, graphite, and fullerene

to be broader than that of diamond, although the main peaks of the carbon allotrope result from the superimposition of 1s-2s2p and 1s-2p2p, respectively. The broader peaks of fullerene and graphite depend upon pπ orbitals of aromatic carbons, since the sharp peak of diamond is due to pσ-orbitals of aliphatic carbons.

Conclusions

We analyzed X-ray photoelectron, and Auger electron spectra of carbon allotrope (diamond, graphite, and C_{60} fullerene) by deMon density-functional theory (DFT) calculations using the model molecules.

(1) The simulated spectra by DFT calculations using the model molecules [adamantane derivative ($C_{10}H_{12}(CH_3)_4$), pyrene ($C_{16}H_{10}$) and fullerene (C_{60})] show good accordance with the experimental ones. For the

fullerene, the experimental spectrum in the range of more than 12 eV is almost similar to that of graphite, although it is characteristic that the spectrum in the range of less than 12 eV has four broader peaks mainly due to the pπ (C2p-C2p) bondings.

(2) Auger electron spectra for the allotrope show good accordance with the experimental ones, although we couldn't also observe the Auger electron spectrum for solid C_{60}. The experimental AES of the allotrope can be classified in each range of 1s-2p2p, 1s-2s2p, and 1s-2s2s transitions for C KVV spectra.

References

[1] K. Endo, T. Morohashi, T. Otsuka, S. Koizumi, M. Suhara, D. P. Chong, J. Surf. Anal., **6**, 186(1999).

[2] K. Endo, S. Koizumi, T. Otsuka, M. Suhara, T. Morohashi, E. Z. Kurmaev, D. P. Chong, J. Comp. Chem., **22**,102(2001).

[3] A. St-Amant, D. R. Salahub, Chem. Phys. Lett., **169**,387(1990); St-Amant A., Ph. D. Thesis, University of Montreal, 1991.

[4] K. Endo, Y. Kaneda, M. Aida, D. P. Chong, J. Phys. Chem. Solids, **56**,1131(1995).

[5] K. Endo, C. Inoue, Y. Kaneda, M. Aida, N. Kobayashi, D. P. Chong, Bull. Chem. Soc. Jpn., **68**,528(1995).

[6] K. Endo, Y. Kaneda, H. Okada, D. P. Chong, P. Duffy, J. Phys. Chem., **100**,19455(1996).

[7] K. Endo, D. P. Chong, J. Surface Anal., **3**,618(1997); ibid., **4**,50(1998).

[8] S. Kuroki, K. Endo, S. Maeda, D. P. Chong, P. Duffy, Polym. J., **30**,142(1998).

[9] J. C. Slater, Advan. Quantum Chem., **6**,1(1972).A. R. Williams, R. A. deGroot, C. B. Sommers, J. Chem. Phys., **63**,628(1975).

[10] A. R. Williams, R. A. deGroot, C. B. Sommers, J. Chem. Phys., **63**,628(1975).

[11] J. F. Janak, Phys. Rev., **A 18**,7165(1978).

[12] P. Duffy, D. P, Chong, Org. Mass. Spectrom., **28**,321(1993).

[13] D. P. Chong, Chem. Phys. Lett., **232**,486(1995).

[14] D. P, Chong, J. Chem. Phys., **103**,1842(1995).

[15] D. P. Chong, C. H. Hu, P. Duffy, Chem. Phys. Lett., **249**,491(1996).

[16] T. Otsuka, K. Endo, M. Suhara, D. P.Chong, J. Mol. Struct., **522**, 47 (2000).

[17] L. Åsbrink, C. Fridh, E. Lindholm, Chem. Phys. Lett., **52**,69(1977).

[18] U. Gelius, K. Siegbahn, Faraday Discus. Chem. Soc., **54**,257(1972): Gelius U., J. Electron. Spectrosc. Relat. Phenom., **5**,985(1974).

[19] J. –J. Yeh, "Atomic Calculation of Photo-ionization Cross Section and Asymmetry Parameters" by Gordon and Breach Science Publishers,1993.

[20] G. Wentzel, Z. Phys., **43**,524(1927).

[21] H. Siegbahn, L. Asplund, P. Kelfve, Chem. Phys. Lett., **35**,330(1975).

[22] D. E. Ramarker, J. S. Murday, N. H. Turner, G. Moore, M. G. Lagally, J. Houston, Phys. Rev. **B 19**,5375 (1979).

[23] D. E. Ramarker, Phys. Rev. **B 21**,4608(1980).

[24] M. H. Chen, F. P. Larkins, B. Crasemann, At. Data Nucl. Data Tables, **45**,1 (1990).

[25] M. J. S. Dewar and E. G. Zoebisch, Theochem., **180**,1(1988); M. J. S. Dewar, E. G. Zoebisch, E. F. Healy, and J. J. P. Stewart, J. Am. Chem. Soc.,**107**,3902(1985).

[26] A. D. Becke, Phys. Rev., **A 38**,3098(1988).

[27] J. P. Perdew, Phys. Rev., **B 33**,8822(1986).

[28] J. C. Angus, C. C. Hayman, Science, **241**, 919(1988).

[29] T. David, J. K. Gimzewski, D. Purdie, B. Reihl, R. R. Schlitter, Phys. Rev., **B 50**,5810 (1994).

[30] J. Onoe, A. Nakao, K. Takeuchi, Phys. Rev., **B 55**,10051(1997).

[31] R.G. Cavell, S.P. Kowalczyk, L. Ley, R.A. Pollak, B. Mill, D. A. Shirley, W. Perry, Phys. Rev., **B7**,5313(1973).

[32] V. G. Aleshi, Yu.N. Kucherenko, J. Electron Spectrosc. Relat. Phenom., **8**,411(1976).

[33] J. S. Murday, B. I. Dunlap, F. L. Hutson II, P. Oelhafen, Phys. Rev., **B24**,4764(1981).